SAE International™

Investigation of Knock Limited Compression Ratio of Ethanol Gasoline Blends

2010-01-0619
Published
04/12/2010

James Szybist
Oak Ridge National Laboratory

Matthew Foster, Wayne R. Moore and Keith Confer
Delphi Powertrain Systems

Adam Youngquist and Robert Wagner
Oak Ridge National Laboratory

ABSTRACT

Ethanol offers significant potential for increasing the compression ratio of SI engines resulting from its high octane number and high latent heat of vaporization. A study was conducted to determine the knock limited compression ratio of ethanol - gasoline blends to identify the potential for improved operating efficiency. To operate an SI engine in a flex fuel vehicle requires operating strategies that allow operation on a broad range of fuels from gasoline to E85. Since gasoline or low ethanol blend operation is inherently limited by knock at high loads, strategies must be identified which allow operation on these fuels with minimal fuel economy or power density tradeoffs.

A single cylinder direct injection spark ignited engine with fully variable hydraulic valve actuation (HVA) is operated at WOT and other high-load conditions to determine the knock limited compression ratio (CR) of ethanol fuel blends. The geometric CR is varied by changing pistons, producing CR from 9.2 to 12.87. The effective CR is varied using an electro-hydraulic valvetrain that changed the effective trapped displacement using both Early Intake Valve Closing (EIVC) and Late Intake Valve Closing (LIVC). The EIVC and LIVC strategies result in effective CR being reduced while maintaining the geometric expansion ratio.

It was found that at substantially similar engine conditions, increasing the ethanol content of the fuel results in higher engine efficiency and higher engine power. These results can be partially attributed to a charge cooling effect and a higher heating value of a stoichiometric mixture for ethanol blends (per unit mass of air). Additional thermodynamic effects on the ratio of specific heats (γ) and a mole multiplier are also explored.

It was also found that high CR can increase the efficiency of ethanol fuel blends, and as a result, the fuel economy penalty associated with the lower energy content of E85 can be reduced by about twenty percent. Such operation necessitates that the engine be operated in a de-rated manner for gasoline, which is knock-prone at these high CR, in order to maintain compatibility. By using early and late intake valve closing strategies, good efficiency is maintained with gasoline, but peak power is about 33% lower than with E85.

INTRODUCTION

There has been a dramatic increase in the use of fuel ethanol in the United States in the past decade, as shown in Figure 1. The ethanol consumption in 2008, 221,637 thousand barrels, was equivalent to 6.7% of the volume of gasoline sold [1]. The Energy Independence and Security Act (EISA) of 2007 [2] requires that production of bio-derived fuels increase more than 7 fold from their 2007 levels by 2020. Thus, production and consumption of fuel ethanol will almost certainly continue to increase rapidly in an effort to comply with EISA.

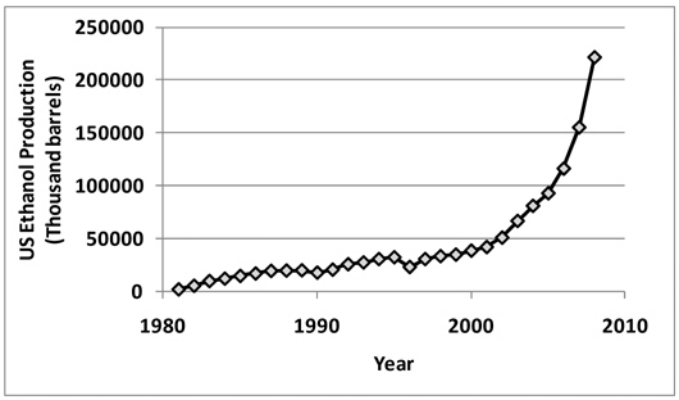

Figure 1. Ethanol production in the United States. Data from the US Energy Information Administration [1].

Two legal forms of ethanol fuel blends are currently sold in the US: E10 and E85. E10, which is nominally 10 vol% ethanol blended with gasoline or gasoline blendstock, can be used in all gasoline vehicles. E85, which can contain nominally from 70 to 85 vol% ethanol [3], is only compatible with Fuel Flexible Vehicles (FFVs). For a more complete assessment of ethanol compatibility, see reference [4]. Approximately 99% of the fuel ethanol sold in the US is in the form of E10, and even if all the gasoline sold in the US contains 10% ethanol, the goals of EISA cannot be met [4]. Thus, the US Department of Energy (DOE) has an interest in increasing the amount of E85 consumed. From a technical perspective there is need to understand the behavior of all intermediate ethanol-gasoline blends up to E85 because in an FFV, gasoline is frequently added to a partial-tank of E85, or visa-versa. The result is that any ethanol blend level can be in the fuel tank of an FFV, from E0 to E85.

One of the market barriers associated with increased consumer use of E85 is reduced fuel economy compared to gasoline. Ethanol blends do not operate any less efficiently than gasoline; on the contrary, as will be discussed in the present study, ethanol blends actually have an increased thermal efficiency. The reduced fuel economy for E85, and other ethanol-gasoline blends, can be attributed to lower energy content on both a mass and volumetric basis. The energy content of E85 is approximately 32% lower than gasoline on a mass basis.

The broad goal of this project is to investigate optimization methodologies for E85 in an effort to minimize the fuel penalty compared to gasoline. The fuel properties of ethanol, in particular the high octane number and high latent heat of vaporization, provide opportunities for higher efficiency with ethanol that are not currently exploited in current FFVs. For the most part, FFVs being offered by automakers are vehicles that are optimized for gasoline but are able to operate with ethanol, including changes in materials, fuel injector delivery rate, and allowances in engine controller algorithms. Recent work shows that this trend is beginning to change, and that optimization for ethanol is approaching [5].

The specific goal of this study is to examine the high-load knock-limits of ethanol blends at three different compression ratio configurations. In doing so, we also investigate the feasibility of maintaining compatibility with lower-octane gasoline using two unconventional valve strategies: early intake valve closing (EIVC) and late intake valve closing (LIVC). Specific interest is paid to power, thermal efficiency, and fuel consumption. Combustion analysis is also discussed. A discussion of the emission measurements will be the topic of a future study, and are not discussed here.

EXPERIMENTAL METHODOLOGY

METHODOLOGY 1: EXPERIMENTAL PLATFORM

This study utilizes a new single cylinder engine apparatus at ORNL equipped with a fully variable hydraulic valve actuation (HVA) system from Sturman Industries. The base engine is a GM 2.0L Ecotec engine with direct fuel injection. The geometry of the engine is listed in Table 1. The engine is equipped with a turbocharger in its production configuration, but is operated as a naturally aspirated engine for this study. Numerous modifications were made to the cylinder head, engine block, intake manifold, and exhaust manifold to allow the engine to accommodate the HVA system and allow it to function as single-cylinder engine.

Table 1. Engine Geometry

Bore	86 mm
Stroke	86 mm
Connection Rod	145.5 mm
Fueling	Direct Injection
Compression Ratio	9.2*, 11.85, and 12.87
Valves per Cylinder	4

**Compression ratio with the production piston*

The modifications made to the cylinder head allow three of the cylinders to be disabled, and accommodate the HVA actuators from Sturman Industries. The engine operates in a camless configuration, so both the intake and exhaust cams have been removed. Valves and springs are left in place for the deactivated cylinders so that they can be sealed. The production fuel pump is driven by the intake cam, thus it cannot be used for a camless engine configuration. Instead, pressurized fuel is sent directly to the fuel rail from a pump cart at 10MPa for this study. The oil passages in and out of the engine head are sealed because the production valve-train lubrication system is not necessary with HVA actuators. Machining modifications allow the cylinder head to

accommodate a transfer plate and the HVA actuators. Custom fabricated intake and exhaust valves with longer valve stems than the production engine are used, a feature needed in order to mate with the HVA actuators. Other than the extended valve stems, the valves are geometrically identical to the production valves. The custom valves are made from stainless steel, unlike the production valves which are sodium-filled, so some heat transfer differences can be expected. The engine operates without a valve cover. The engine and the modified head can be seen in Figure 2.

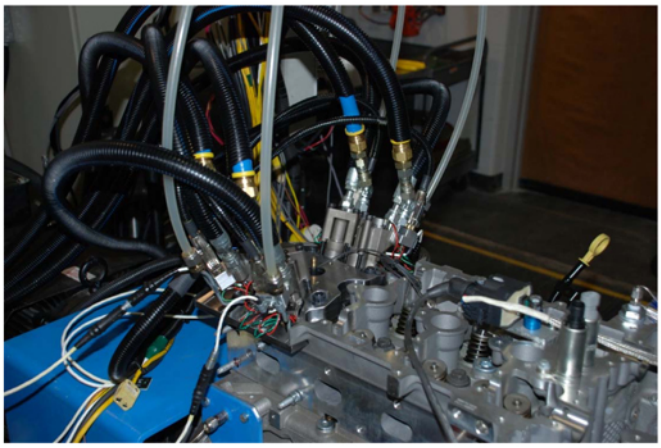

Figure 2. Modified cylinder head with installed HVA actuators.

HVA research modules from Sturman Industries are used to allow a high degree of valve event flexibility. The valve opening and closing timing as well as the valve lift can be controlled independently for each of the four valves. Valve lift can be controlled from 1.2 to 9.3mm and valve events resemble square waves, with rapid valve opening, a constant valve lift dwell, and rapid valve closing. Rate shaping of the valve events to resemble a cam profile cannot be performed and only one valve lift setpoint per valve event is permitted. Thus, while low-lift valve events can occur at or near piston TDC, the permitted timing of higher lift valve events are restricted to prevent valve-piston collisions. The effective consequence of this limitation is that overlap of the intake and exhaust valve events is not permitted for high valve lift conditions.

Cylinders 1, 2, and 3 are disabled by machining holes into the pistons and removal of the piston rings, which together serve to prevent compression and to reduce friction. A picture of the modified pistons installed in the engine is shown in Figure 3. Added weight to the wristpin replaces the weight removed by machining the piston for balancing purposes. The oil pump integrated into the crankcase is used without modification, and an electric water pump is used to circulate coolant.

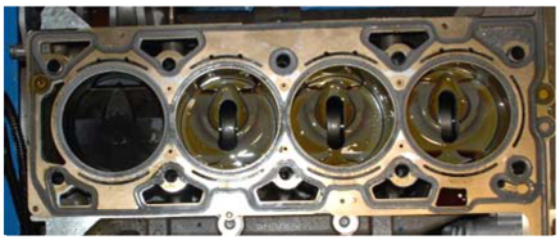

Figure 3. Pistons that have been modified for the deactivated cylinders.

A flexible open engine controller from Drivven Inc. is used for engine management. The engine controller uses electronic components from National Instruments as well as Drivven Inc. The engine controller program uses the LabVIEW software programming environment, including the RealTime and the Field Programmable Gate Array (FPGA) add-in modules. The controller is configured to control spark, fuel, and throttle. An added software package in the engine controller, Drivven Combustion Analysis Toolkit (DCAT), performs the crank-angle resolved data acquisition and combustion analysis. Crank-angle resolved measurements include cylinder pressure, valve lift feedback from each of the four valves, and current sent to the fuel injector.

The intake manifold is modified to block the intake runners to the disabled cylinders, as can be seen in Figure 4. As can also be seen in Figure 4, the intake manifold is fitted with an aftermarket port fuel injector, which was not used in this study but does provide this engine experiment with an added element of flexibility which will be used in future studies.

<figure 4 here>

Cylinder pressure measurements are performed using a piezoelectric pressure transducer integrated into a sparkplug. In order to accommodate the need for increasing spark energy at higher CR, a higher energy ignition coil was used at the highest compression ratio (CR), but both were coil-near-plug inductive ignition systems. The production DI fuel injectors were used. An encoder with a resolution of 1800 pulses per revolution was used for both crank-angle resolved data acquisition, and for engine and valve control.

METHODOLOGY 2: COMPRESSION RATIO CONFIGURATIONS

A series of custom pistons were designed and fabricated to change the geometric CR of the engine. In addition to the production piston, which produces a CR of 9.2, two additional pistons are investigated, with resultant CR of 11.85 and 12.87. An attempt was made to operate a fourth piston, with a resultant CR of 13.66, but reliable ignition could not be achieved. The series of pistons is shown in Figure 5.

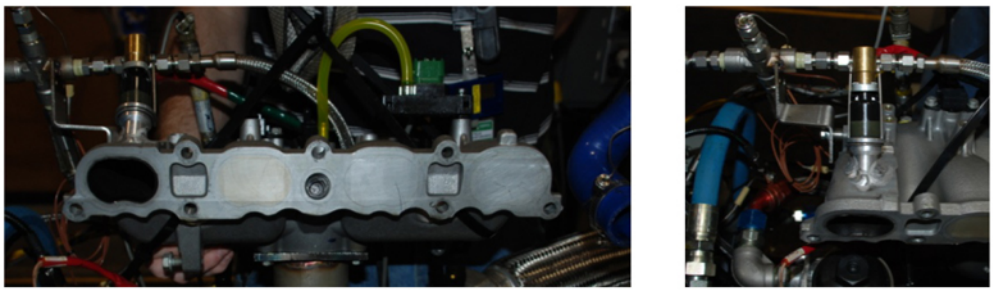

Figure 4. Modified intake manifold blocked intake runners and an added port fuel injector.

Figure 5. Series of pistons and resultant compression ratios investigated.

<figure 5 here>

The higher CR pistons result in reduced valve clearance. In order to prevent collisions between the piston and valves, reduced clearances necessitate an earlier exhaust valve closing (EVC) and a later intake valve opening (IVO) angle. In order to maintain consistency for all CR configurations, EVC was held constant at 345 crank angle (CA) and IVO was held constant at −344 CA, where 0 CA represents combustion TDC.

METHODOLOGY 3: FUELS

A total of 5 fuels are investigated in this study: regular gasoline (RG), high octane gasoline (HO), and ethanol blends of 10% (E10), 50% (E50), and 85% (E85). Both RG and HO are emissions certification gasolines from Chevron Phillips Chemical Company LLC (CPChem) with product names UTG-91 and UTG-96, respectively.

Ethanol blends are prepared by splash blending in-house using RG and denatured fuel-grade ethanol blendstock (E100), also from CPChem. Selected fuel properties are shown in Table 2.

<table 2 here>

It is interesting to note that the blending response of RON and MON as a function of ethanol content is highly non-linear. There is a substantial octane improvement between RG and E10, and between E10 and E50. However, between E50 and E85 there is very little difference in either RON or MON. It is well-established that properties of ethanol-gasoline blends, such as Reid vapor pressure, do have non-linear responses [4]. Surprisingly, the authors have been unable to find RON and MON measurements as a function of ethanol content that either support or refute these results.

The decision to use RG as the blend stock for ethanol blending, rather than HO, was based on real-world trends in that ethanol is unlikely to be blended with high-octane gasoline. As fuel ethanol consumption increases in the US, there is a trend away from splash-blends toward match-blends, which use a blendstock for oxygenate blending (BOB). In splash-blending, ethanol is mixed with a finished in-spec gasoline, whereas with match blending the ethanol is blended with a BOB that is formulated for the specific purpose of ethanol blending. One of the intended purposes of BOB is to reduce evaporative emissions by reducing the vapor pressure of ethanol fuel blends. Importantly, since ethanol also acts as an octane improver, the octane number of BOB doesn't need to be as high as conventional finished gasoline to meet market specs. Because producing a high octane product is more expensive for refiners, the BOB blendstock is likely to be of a lower octane than conventional gasoline. Thus, the ethanol fuels for this study were blended with the lower-octane gasoline.

Table 2. Properties of investigated fuel matrix.

Fuel Property	Test Method	RG	HO	E10	E50	E85
Research Octane Number (RON)	ASTM D2699	90.8	96.1	95.7	101.6	101.5
Motor Octane Number (MON)	ASTM D2700	82.8	87	85.3	89.5	90.1
Antiknock Index (R+M)/2	N/A	86.8	91.6	90.5	95.6	95.8
Wt. % C	ASTM D240	86.3	86.5	81.98	68.58	56.71
Wt. % H	ASTM D240	13.7	13.5	13.28	13.19	12.97
Wt. % O	ASTM D240 by difference	0	0	4.74	18.23	30.32
Stoichiometric Air-Fuel Ratio	N/A	14.56	14.55	13.71	11.57	9.61
Specific Gravity	ASTM D 4052	0.7305	0.7400	0.7456	0.8	0.7855
Lower Heating Value (MJ/kg)	ASTM D240	43	42.8	41.5	34.8	29.2
Reid Vapor Pressure (psia)	ASTM D5191	9	9	9.9	8.3	5.6
Ethanol Content (vol%)	ASTM D5599	n/a	n/a	11.2	51.3	87.2

**Reported property values for RG and HO are for typical values of these products. Actual values of this batch were not measured.*

METHODOLOGY 4: EXPERIMENTAL PROCEDURE

The investigation consisted of ten engine operating conditions per fuel per compression ratio, resulting in a matrix of 10×5×3 = 150 points, although a number of these proved to be inoperable. Each operating point consisted of a spark sweep to locate the maximum brake torque (MBT) spark timing. All fuels were run at stoichiometric conditions. A graphical representation of the engine operating conditions is shown in Figure 6.

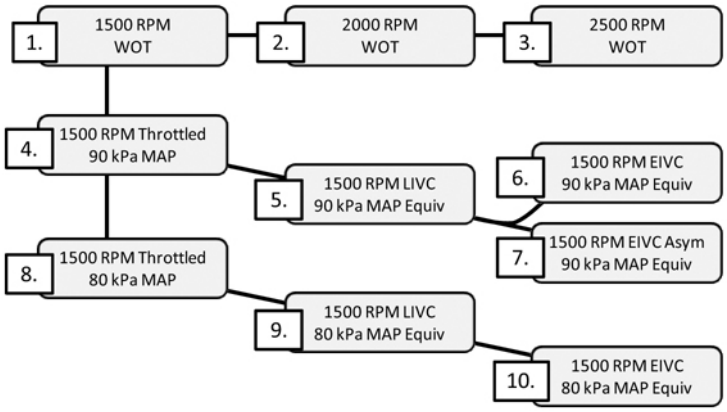

Figure 6. Engine operating conditions investigated.

Engine operating points 1, 2, and 3 represent a speed sweep at full engine load, from 1500 to 2500 rpm. Engine operating points 1, 4, and 8 represent a load sweep, accomplished by throttling, at 1500 rpm. Engine operating points 1, 2, 3, 4 and 8 all share common valve timing conditions. Engine operating conditions 5, 6, and 7 have the same fuel and air flow rates as point 4 for a given fuel and CR, but operate unthrottled with valve events controlling air flow instead of throttling, thus they are designated as equivalent to the 90 kPa throttled condition for comparison. Similarly, points 9 and 10 have the same air and fuel flow rate as point 8 for a given fuel and CR, but operate unthrottled and with unconventional valve events to control air flow, making them equivalent to the 80 kPa MAP throttled condition for comparison. Points 5 and 9 utilize a late intake valve closing (LIVC) strategy to control air flow, breathing excess air into the cylinder during the intake stroke, and then discharging a portion of it back into the intake manifold during the beginning of the compression stroke. Points 6, 7, and 10 utilize an early intake valve closing (EIVC) strategy where the intake valve is closed during the latter portion of the intake stroke, trapping only the desired mass of air, resulting in the remainder of the intake stroke creating a vacuum in the cylinder. Operating point 7 differs from point 6 in that the closing angles for the two intake valves are different, producing an asymmetric profile. The asymmetric intake valve closing is done in an effort to induce charge motion to reduce combustion duration, with one intake valve closing 60 crank angle degrees before the other. Both the LIVC and EIVC strategies have been investigated previously as methods of operating the engine unthrottled for higher efficiency [6, 7]. While that is true here, we are also investigating the feasibility of these strategies to mitigate knock.

Valve lift is 9 mm for both the intake and exhaust valves for all operating conditions except for the asymmetric early intake case (operating condition 7). For this conditition, the duration of the shorter valve event is too short for the valve to fully open to 9 mm, and achieving the valve lift setpoint is required for the Sturman valve system. Thus, the intake valve lift at this operating condition is reduced to 5 mm.

It was desirable to inject the fuel during the intake stroke to ensure good mixing. The start of fuel injection for operating points 1-5 as well as 8 and 9 is −270 CA, where 0 CA represents combustion TDC. The start of injection timing was advanced to −300 CA for the EIVC operating points 6, 7, and 10 in an effort to ensure that fuel injection occurred near maximum lift of the intake stroke, and not near intake valve closing. Start of injection timing was held constant for all fuels at a given operating point.

RESULTS AND DISCUSSION

The MBT spark timing, indicated mean effective pressure (IMEP), indicated specific fuel consumption (ISFC) and indicated thermal efficiency (ITE) are shown in Table 3. For the purposes of this study, all references to IMEP refer to net IMEP, and similarly ISFC and ITE are calculated using the net IMEP. As expected, the factors that contribute to increased knock are decreased RON and MON, increased compression ratios, increased engine load, and decreased engine speed. In some cases, spark advance is knock-limited, resulting in an efficiency penalty. In other cases, knock was so severe that the engine condition is inoperable. Because of temperature considerations in the exhaust manifold, the most retarded spark timing considered for this work is 0 CA, or TDC.

As stated in the Introduction section, emissions measurements were performed during this set of experiments but are not presented here because they will be the subject of a future paper. However, the differences in engine performance are not the result of major differences in mixture preparation and combustion efficiency. Combustion efficiency variation throughout the experiment was low, with a range of 94.6% to 96.7%.

Table 3 contains a large amount of information about the effects of fuel composition, CR, and valve events on efficiency, ISFC, and IMEP. The shading of the inoperable and knock-limited cases serves as a visual indication of operability limitations as CR is increased, and throughout the remainder of this paper, the data in Table 3 is analyzed, plotted and discussed in detail. The data in Table 3 is provided primarily to serve as a data reference throughout the remainder of the paper.

CR, FUEL, AND VALVE TIMING EFFECTS ON ISFC AND EFFICIENCY

CR Effects on ISFC and Efficiency

A First Law Thermodynamic analysis tells us that the efficiency of an air-standard Otto Cycle is fundamentally related to CR according to the following relationship [8]

$$\eta = 1 - \left(\frac{1}{CR}\right)^{\gamma - 1}$$

Equation 1

where η is thermal efficiency and γ is the ratio of constant pressure to constant volume heat capacity, a term that is discussed in more depth in the next section. Heywood explains that experimental results agree with fundamental thermodynamics, with increased CR producing higher efficiency, but also show diminishing efficiency returns with CR > 14 due to higher heat and friction losses [9]. In practice, CR in production engines is limited by the ability of gasoline to resist knock, especially at the most knock-prone engine conditions which are low-speed and high-load.

High ethanol blends have been shown to permit higher CR operation. Caton et al. [10] showed that for E85 blends, the maximum brake torque (MBT) spark timing could be maintained up to a CR of about 13.5, whereas MBT could not be maintained for gasoline and E10 past a CR of 9.0 in a modified CFR octane rating engine. Nakata et al. [11] showed at a CR of 13.0, MBT timing was knock-constrained for E0, E10, and E20, but not knock-constrained for E50 and E100 at the tested conditions. Stein et al. [12] evaluated a dual fuel system, where gasoline was delivered through a PFI injector as the primary engine fuel, and E85 was delivered as the secondary engine fuel as-needed to prevent knock. It was found that under turbocharged conditions with a 12.0 CR configuration, the maximum amount of E85 required to prevent knock at peak load was less than 60%, which is effectively about E50. The work here is unique in that it investigates, in combination, the effect of several high CR in an engine with DI fueling and with ethanol blends.

<table 3 here>

Figure 7 shows ITE, ISFC, and IMEP as functions of compression ratio for E85 and RG at two different operating conditions (condition 3, 2500 rpm WOT, and condition 9, 1500 rpm LIVC, 80 kPa equiv). For E85, which isn't knock-limited at either of these operating condition, ITE and IMEP both increase with increasing CR, while ISFC decreases. However, the spark advance for RG is limited for both of these operating conditions at CR > 9.2. Thus, spark timing is retarded to prevent knock for RG. Previous work has quantified a power penalty and an efficiency penalty associated with retarded spark timing [13], a penalty that holds true here for RG. As a consequence, Figure 7 shows that the peak ITE is achieved at a CR lower than the peak CR. In addition, unlike E85, RG does not exhibit a consistent increase in IMEP as CR increases, a result that can also be attributed to spark retard.

Thus, these results show that increased CR does provide a substantial ITE increase when spark advance is not knock-limited. For fuels that are knock-limited, increasing CR

Table 3. MBT spark timing, ISFC, IMEP, and thermal efficiency for all operating conditions. Shaded points are knock-limited and blacked out points are inoperable.

	1. 1500 RPM WOT				2. 2000 RPM WOT				3. 2500 RPM WOT				4. 1500 RPM Throttled 90 kPa MAP				5. 1500 RPM LIVC 90 kPa MAP Equiv			
	Spark	ISFC	ITE	IMEP	Spark	ISFC	ITE	IMEP	Spark	ISFC	ITE	IMEP	Spark	ISFC	ITE	IMEP	Spark	ISFC	ITE	IMEP
	CA BTDC	g/kW-h	%	kPa	CA BTDC	g/kW-h	%	kPa	CA BTDC	g/kW-h	%	kPa	CA BTDC	g/kW-h	%	kPa	CA BTDC	g/kW-h	%	kPa
9.20 Compression Ratio																				
RG	10	233.6	35.8	1028.2	13	230.1	36.4	1081.8	17	229.0	36.5	1024.6	13	239.8	34.9	871.2	14	235.2	35.6	892.1
HO	13	228.7	36.8	1056.6	14	229.9	36.6	1103.3	17	226.4	37.2	1031.9	14	238.3	35.3	890.8	14	235.4	35.7	921.3
E10	13	241.1	36.0	1055.6	15	236.9	36.6	1111.0	18	231.0	37.5	1042.0	13	245.0	35.4	895.9	15	242.3	35.8	915.9
E50	14	278.6	37.1	1101.9	15	277.2	37.3	1151.2	21	279.1	37.1	1067.1	16	288.5	35.9	937.0	16	285.2	36.3	949.1
E85	16	326.2	38.0	1116.2	17	324.6	38.2	1171.5	17	315.7	39.3	1092.0	15	336.3	36.9	954.0	15	332.3	37.3	979.0
11.85 Compression Ratio																				
RG					3	239.5	34.9	1053.4	7	229.9	36.4	1040.9	2	247.7	33.8	870.6	6	232.7	36.0	915.1
HO	5	235.1	35.8	1048.0	8	227.1	37.0	1119.4	12	219.7	38.3	1076.3	7	235.4	35.7	926.0	10	229.0	36.7	942.7
E10	3	253.5	34.2	1022.2	8	237.7	36.5	1105.0	13	231.4	37.5	1070.5	6	254.8	34.0	897.6	8	243.4	35.6	930.4
E50	14	270.4	38.3	1142.9	14	269.6	38.4	1196.4	18	264.7	39.1	1121.9	13	275.1	37.6	979.3	15	271.9	38.0	979.4
E85	14	317.7	39.0	1155.1	15	318.5	38.9	1205.1	18	303.4	40.9	1135.2	14	323.9	38.3	987.5	12	322.2	38.5	997.7
12.78 Compression Ratio																				
RG									3	240.5	34.8	1022.8								
HO					5	233.1	36.1	1107.4	8	218.1	38.6	1110.4	2	240.7	34.9	917.0	5	225.7	37.3	966.8
E10					4	250.6	34.6	1093.6	8	229.0	37.8	1107.4	2	254.8	34.0	917.7				
E50	11	261.8	39.5	1195.8	12	257.8	40.1	1261.9	13	255.6	40.5	1196.4	9	270.1	38.3	1003.6	11	265.9	38.9	1011.7
E85	11	301.9	41.1	1237.5	13	298.1	41.6	1301.8	16	291.3	42.6	1247.5	11	307.8	40.3	1041.2	13	303.6	40.8	1048.4

	6. 1500 RPM EIVC 90 kPa MAP Equiv				7. 1500 RPM EIVC Asym 90 kPa MAP Equiv				8. 1500 RPM Throttled 80 kPa MAP				9. 1500 RPM LIVC 80 kPa MAP Equiv				10. 1500 RPM EIVC 80 kPa MAP Equiv			
	Spark	ISFC	ITE	IMEP	Spark	ISFC	ITE	IMEP	Spark	ISFC	ITE	IMEP	Spark	ISFC	ITE	IMEP	Spark	ISFC	ITE	IMEP
	CA BTDC	g/kW-h	%	kPa	CA BTDC	g/kW-h	%	kPa	CA BTDC	g/kW-h	%	kPa	CA BTDC	g/kW-h	%	kPa	CA BTDC	g/kW-h	%	kPa
9.20 Compression Ratio																				
RG	23	235.3	35.5	878.2	18	234.7	35.6	883.8	14	244.4	34.2	749.1	15	237.2	35.3	777.0	29	235.4	35.5	769.9
HO	25	231.0	36.4	915.1	20	232.9	36.1	916.5	16	243.9	34.5	752.8	16	232.4	36.2	776.6	30	232.5	36.2	778.5
E10	25	237.5	36.5	916.9	21	240.3	36.1	913.0	15	253.7	34.2	762.1	17	243.1	35.7	786.0	29	241.3	35.9	785.0
E50	24	283.1	36.5	937.5	21	285.1	36.3	937.0	15	295.9	35.0	788.5	16	285.6	36.2	810.8	31	286.0	36.2	806.9
E85	27	326.0	38.0	970.9	23	325.2	38.1	966.9	15	337.9	36.7	819.7	17	330.0	37.6	833.5	26	332.0	37.3	825.2
11.85 Compression Ratio																				
RG	13	233.9	35.8	891.6	6	242.9	34.4	875.6	5	248.3	33.7	774.6	11	228.0	36.7	813.8	21	228.9	36.6	808.5
HO	18	227.5	37.0	937.6	12	230.5	36.5	927.5	9	240.0	35.0	800.3	14	226.9	37.1	822.8	28	225.5	37.3	820.5
E10	18	244.7	35.4	913.1	10	245.7	35.3	907.3	8	255.6	33.9	785.8	13	240.5	36.0	809.8	25	241.9	35.8	808.0
E50	24	272.0	38.0	991.7	20	269.8	38.3	996.1	13	283.3	36.5	833.6	15	274.6	37.7	845.5	28	275.7	37.5	841.6
E85	23	320.3	38.7	999.1	22	316.6	39.2	1020.2	14	333.0	37.2	838.9	14	323.4	38.3	855.1	28	326.0	38.0	834.5
12.78 Compression Ratio																				
RG									1	246.4	34.0	787.8	5	228.1	36.7	831.8	12	229.1	36.5	820.6
HO	10	228.9	36.7	952.2	8	229.5	36.7	943.0	4	237.4	35.4	799.0	8	224.2	37.5	845.8	19	221.2	38.0	847.2
E10	10	243.2	35.6	946.9	6	249.3	34.8	928.6	4	252.5	34.3	813.1	8	238.2	36.4	852.9	18	239.7	36.2	843.8
E50	20	266.3	38.9	1013.0	15	269.6	38.4	1004.8	10	276.6	37.4	862.8	11	268.3	38.6	884.1	24	270.7	38.2	875.9
E85	20	307.4	40.3	1041.4	19	297.7	41.6	1065.7	11	314.8	39.4	891.6	13	305.0	40.7	906.5	25	312.5	39.7	904.4

results in an eventual ITE decrease because of retarded spark timing. These results agree with references [10, 11, 12] discussed previously. Also noteworthy in Figure 7 is the observation that at a given operating condition, E85 produces more power and operates more efficiently than RG, even at CR = 9.2 where RG is not knock-limited. This observation is discussed in more depth in the following section. The higher efficiency of E85 is not sufficient to compensate for its reduced energy content relative to RG, thus there is still significantly higher fuel consumption for E85.

<figure 7 here>

Fuel Effects on Power and Efficiency

Changing fuel composition can increase power and efficiency in two ways: by making optimum engine conditions possible, such as in the above discussion where spark advance is knock-limited for RG, or by increasing the power or efficiency of substantially similar engine conditions. The former is largely associated with points that are knock limited for a given fuel. The latter, efficiency and power differences at substantially similar engine conditions, is discussed here.

ITE, IMEP, and ISFC are shown in Figure 8 for each fuel at operating condition 8 (1500 RPM, throttled, 80 kPa manifold pressure) and CR = 9.2. As with Figure 7, this is a subset of the data shown in tabular form in Table 3. Figure 8 is qualitatively representative of all engine conditions at a given CR where spark advance is not knock-limited for any of the fuels. While these operating conditions are substantially similar, with the intake manifold throttled to 80 kPa for all fuels, the trend in net IMEP shows that power output increases with increasing ethanol content. Relative to RG, the IMEP for E85 increases 9.5%, from 749 kPa for RG to 820 kPa for E85. Similarly, ITE also increases with ethanol content, from 34.2% for RG to 36.7% for E85. While this is a

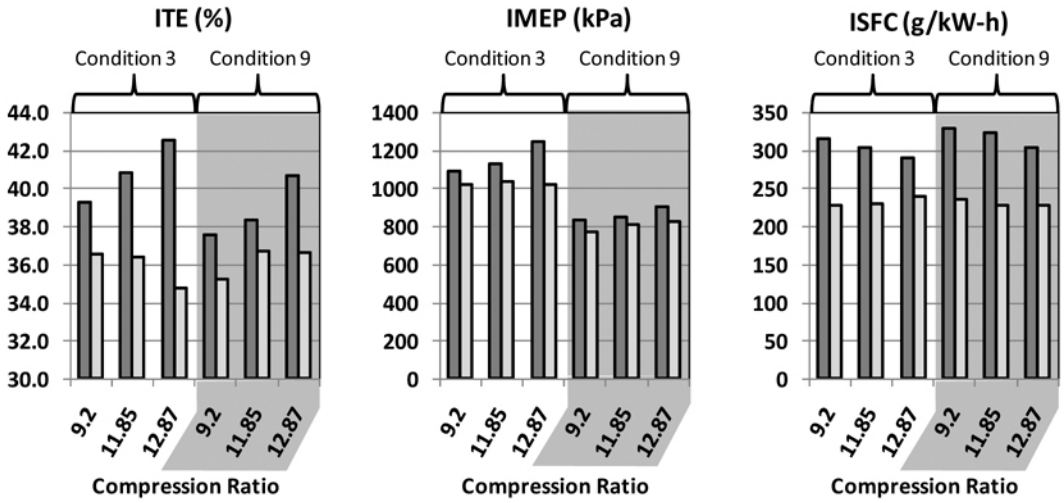

Figure 7. Thermal efficiency, IMEP, and ISFC as functions of CR for (■) E85 and (□) RG at Operating Condition 3 (2500, WOT) and Operating Condition 9 (1500 rpm LIVC, 80 kPa Equiv).

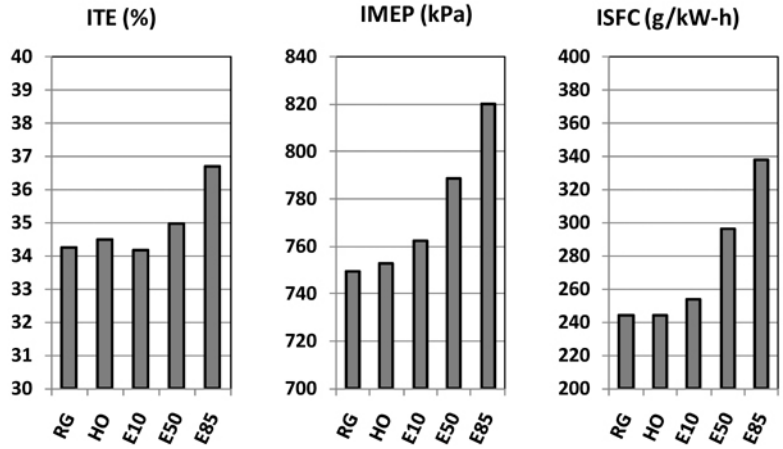

Figure 8. Thermal efficiency, net IMEP, and ISFC for CR = 9.2 and operating point 8 (intake manifold throttled to 80 kPa).

substantial efficiency improvement, it is not sufficient to compensate for the lower energy content of E85 as is seen by an ISFC increase from 244 g/kW-h for RG to 338 g/kW-h for E85.

<figure 8 here>

Thus, with increasing ethanol content, both power and thermal efficiency increase simultaneously. This effect has been noted previously on both engine studies [14] and vehicle studies [15], but while the trend is consistent, it is not fully understood. One contributing factor to the increased power is a charge cooling effect, which increases volumetric efficiency. The average normalized air flow for each of the fuels across all operating points is shown in Figure 9. The airflow for E85 increases about 2% compared to RG, and E50 air flow increases about 1.5%. The increased air flow can be attributed to a charge cooling effect with ethanol due to its higher latent heat of vaporization (919 kJ/kg for chemically pure ethanol, and as 350 kJ/kg for typical gasoline[16]). The mechanism of the charge cooling effect is that when fuel is sprayed into the intake air charge of an engine, the heat needed to vaporize the fuel must be extracted, at least partially, from the air, reducing the specific volume of the intake charge. This is particularly true in an engine with DI fueling, where the fuel has less interaction with the hot engine surfaces in the intake manifold. Since the latent heat of vaporization is significantly higher for ethanol, it is more effective at cooling the intake charge than gasoline.

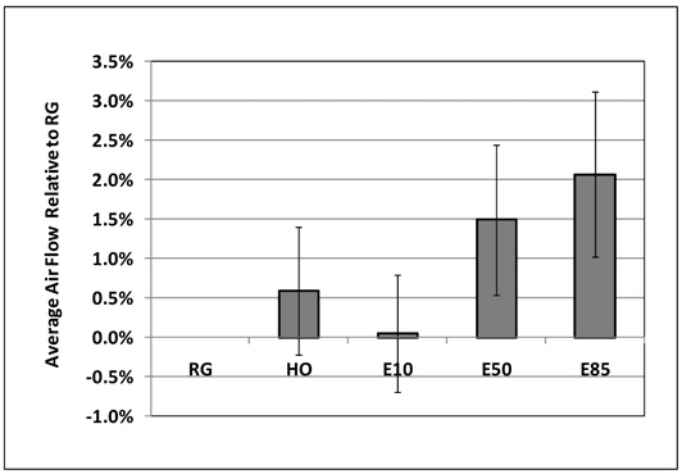

Figure 9. Air flow for operating conditions 4 through 10 at CR = 11.85 for each fuel. Error bars represent standard deviation from all operating points.

The 2% increase in air flow for E85 equates to more than a 2% increase in fuel energy flux for E85. Using the fuel properties presented in Table 2, the heating value of a stoichiometric mixture, per unit mass of air, is calculated and presented in Table 4. The data shows that energy content per unit mass of air increases as ethanol content increases, equating to about a 3.4% increase for E85. Thus, multiplying 102% of the air flow for E85, relative to RG, and 103.4% of the energy content per unit mass of air, the energy flux of E85 is expected to be 105.5% of RG, which accounts for a little over half of the IMEP increase for E85 in Figure 8. It should be noted that the higher energy content of E10 compared to E50 in Table 4 is not thought to be a real phenomenon. Rather, it is thought to be a result of measurement error in either the heat of combustion measurement (ASTM D240) or the elemental analysis measurement (ASTM D5291), both of which are used for this calculation.

Table 4. LHV of stoichiometric mixture per unit mass of air.

Fuels	LHV	Difference
	kJ/g air	%
RG	2.96	0.00%
HO	2.95	-0.37%
E10	3.02	2.28%
E50	3.01	1.78%
E85	3.06	3.35%

With roughly half of the increased IMEP being accounted for with the increased air flow and the increased energy content of a stoichiometric mixture per unit mass of air, the remaining increase in power can be attributed to the higher engine efficiency for ethanol fuels. The additional fuel-specific factors that lead to an increase in efficiency are differences in γ and a mole multiplier (MM) effect. To explore these further, we use the first law of thermodynamics to describe the expansion or compression work for a gas in a reversible adiabatic system gas in Equation 2 from reference [8]

$$\frac{W}{n} = -\frac{R \cdot T_1}{\gamma - 1} * \left[\left(\frac{P_2}{P_1}\right)^{(\gamma-1)/\gamma} - 1\right]$$

Equation 2

where R is the universal gas constant, n is the number of moles, T1 is the initial temperature, and P1 and P2 are the initial and final pressures, respectively. Using relationships between volume, temperature, and pressure, also from reference [8], the pressure terms in Equation 2 are substituted with volume terms in Equation 3, where V1 and V2 are the initial and final volumes. This makes the equation more applicable to engines which have a fixed displacement and clearance volumes.

$$W = -\frac{n \cdot R \cdot T_1}{\gamma - 1} * \left[\left(\frac{V_1}{V_2}\right)^{\gamma-1} - 1\right]$$

Equation 3

The amount of work needed for compression and the amount of work that can be extracted by expansion are dependent on γ. For compression, less work is required for a given ΔV as γ decreases. From an efficiency standpoint, though, it is desirable to have high γ because Otto cycle efficiency improves, as described in Equation 1. This is because when more work is done on the working fluid during compression, the end of compression temperature and pressure are higher, resulting in a greater ΔP during combustion, and more net work out. However, for expansion work, it is desirable to have a low γ. A low γ during expansion maximizes work output from a given starting temperature and pressure condition, as described in Equation 2.

The MM effect impacts the n term in Equation 2. It accounts for the change in the number of moles during the combustion process, and is defined as the ratio of the number of product moles ($n_{products}$) to the number of reactant moles ($n_{reactants}$). From an efficiency standpoint, it is advantageous to have the MM as high as possible so that more moles are available to extract heat from during the expansion process. It should be noted that standard combustion analysis methodologies do not account for an increase in the number of in-cylinder moles. As a result, there is an inherent error in the calculation of in-cylinder temperature, which is calculated from the pressure trace.

In order to quantify both γ and the MM effect, we discuss surrogate fuels that have known molecular weights instead of the real fuels used in this study, specifically iso-octane,

toluene, and ethanol. By balancing the stoichiometric equations for these fuels, as is shown below, the composition during both compression and expansion (assuming the complete stoichiometric products) are known. Using thermodynamic data from reference [17], γ is calculated as a function of temperature and is shown in Figure 10.

Iso-octane: $C_8H_{18} + 12.5\ (O_2 + 3.76N_2) \rightarrow 8CO_2 + 9H_2O + 47N_2$

Toluene: $C_7H_8 + 9\ (O_2 + 3.76N_2) \rightarrow 7CO_2 + 4H_2O + 33.84N_2$

Ethanol: $C_2H_6O + 3\ (O_2 + 3.76N_2) \rightarrow 2CO_2 + 3H_2O + 11.28N_2$

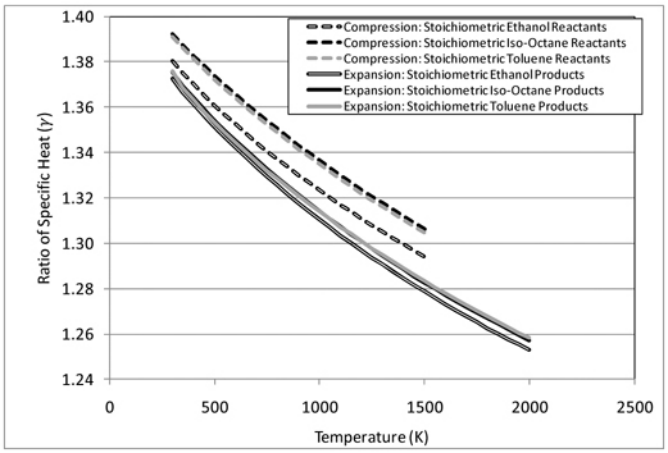

Figure 10. γ as a function of temperature for stoichiometric air/fuel reactants (left side of reaction) and complete stoichiometric products (right side of reaction) of ethanol, iso-octane, and toluene with air.

For stoichiometric mixtures of iso-octane and toluene, the γ values are nearly identical during both compression where the maximum difference is 0.13%, and during expansion, where the maximum difference is 0.08%. Stoichiometric mixtures of ethanol exhibit more variation, being up to 1% lower than iso-octane during compression, and 0.33% lower during expansion. As described above, the lower γ for ethanol during compression is undesirable from an efficiency standpoint, but the lower γ during expansion is desirable. So, while it is clear that there are differences in γ between ethanol and gasoline-range hydrocarbons, the net effect on efficiency is not obvious.

Simply by counting ($n_{products}$) and ($n_{reactants}$) for the balanced stoichiometric equations above, as well as for other similar fuels, Figure 11 is produced to show the MM for a series of alkanes, alcohols and aromatics. Because the molecular formula determines stoichiometry and the MM, n-alkanes and iso-alkanes yield the same result. Within a given class of compounds, there is a consistent trend of increased MM as the MW increases. Each class of compounds exhibits a unique trend, with aromatics having the lowest MM at a given MW, followed by alkanes, and alcohols having the highest. Although olefinic compounds are not shown here, they fall between paraffins and aromatics. In order to calculate the MM for gasoline the exact composition of the fuel must be known. However, we know that gasoline is comprised of a mixture of aromatics, alkanes, and olefins. Thus, an estimate for the MM of gasoline is shown by the shaded region in Figure 11. Thus, the higher MM for ethanol, as well as other alcohols, is advantageous for efficiency.

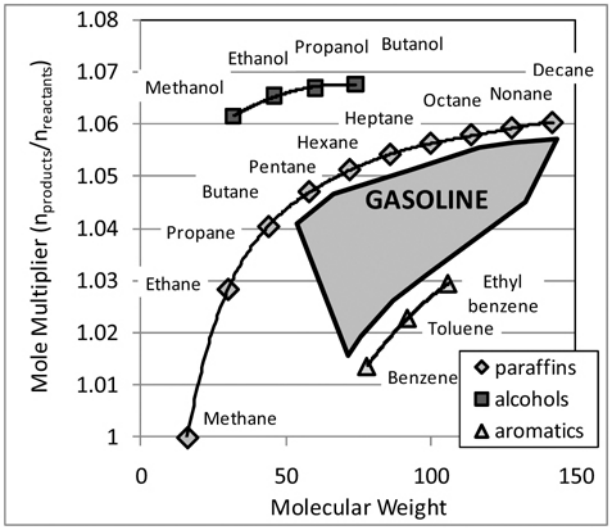

Figure 11. Mole multiplier as a function of molecular weight for alcohols, n-paraffins, and aromatics.

While it is clear that the lower γ and the higher MM may affect thermal efficiency of ethanol-blends, the mechanisms and contributions of these effects are not entirely understood. We can theorize that the mechanism by which the MM can affect efficiency may be through heat transfer. The ideal gas law describes that P = nRT/V, and if we consider P, R, and V to be constant, we see that n and T have an inverse relationship. The implication here is that because ethanol fuels have a higher MM, the temperature required for a given cylinder pressure is lower, and lower temperature will result in less heat transfer to the combustion chamber walls. Supporting this theory are several studies that have found less heat and/or exergy transfer for ethanol-containing fuels [5, 18, and 19]. However, providing a clear understanding of the effects of γ and the MM effect are beyond the scope of this study.

Valve Timing Effects on Efficiency and ISFC

Our application of EIVC and LIVC valve events, rather than throttling, serves two purposes: to control load in a manner that reduces or eliminates engine throttling losses, and to accommodate knock-prone fuels by reducing the effective

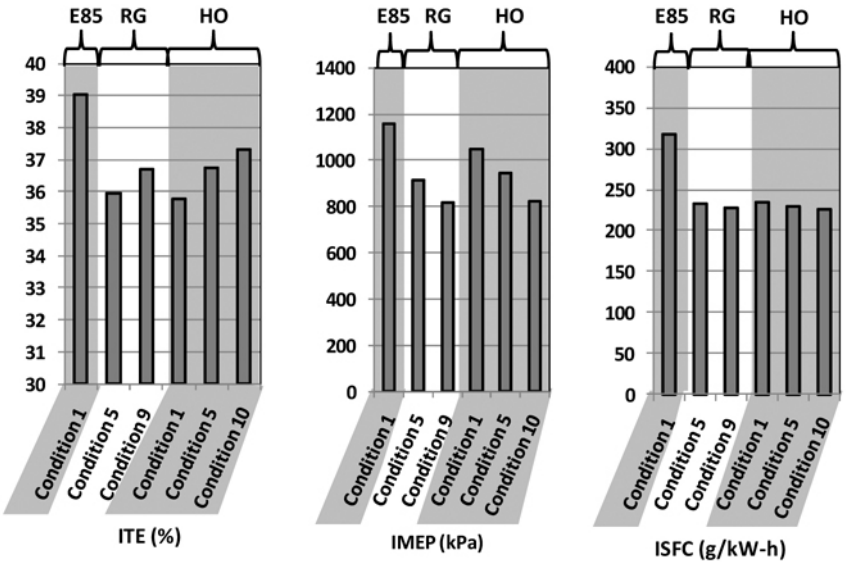

Figure 13. The effects of the possible operating conditions for E85, RG, and HO on thermal efficiency, IMEP, and ISFC when maximum load is demanded at 1500 RPM and CR = 11.85.

CR. Figure 12 presents a schematic of the decision-making methodology.

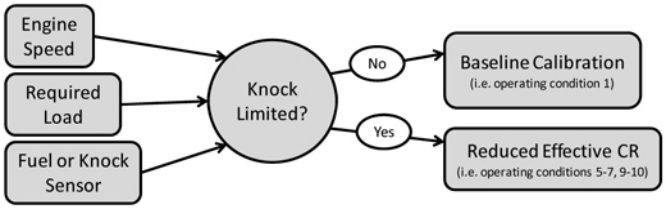

Figure 12. Schematic of use of reduced effective CR to eliminate engine knock.

An example case of this methodology can be taken at a mechanical CR = 11.85, an engine speed of 1500 rpm, and a demand for maximum engine load (i.e. operating condition 1, 1500 RPM WOT). Table 3 shows that this condition is inoperable for the lowest octane fuel (RG), knock-limited for the next two lowest octane fuels (HO and E10), but is not knock-limited for the two highest octane fuels (E50 and E85). Figure 13 shows engine performance for E85 at this condition compared to the possible operating conditions for RG and HO. Compared to E85, the lower octane gasoline, RG, must operate at a lower load. The options are operating condition 5, which offers the highest power output, and operating condition 9 which offers the highest efficiency. Both options impose IMEP reductions (21% and 30%, respectively) and ITE is also reduced. For the higher octane gasoline, HO, the engine is able to operate at condition 1, enabling it to produce a higher power than the lower octane gasoline although is still decreased by 9% compared to E85, and the retarded spark timing negatively affects ITE. Higher efficiency/lower power alternatives for HO are operating conditions 5 and 10, as shown in Figure 13.

<figure 13 here>

Thus, at a high mechanical CR, the fuels that are knock-limited can still be operated, but in a de-rated manner. At 1500 RPM and CR = 11.85, the maximum load for RG, which was the most knock-prone of the fuels tested, represents a 21% reduction in IMEP compared to E85, and the ITE is reduced from 39.0% to 36.0%. For HO, which is knock-limited but operable at WOT with a retarded spark timing, the highest power output results in a 9% reduction in IMEP and a reduction in ITE to 35.8% compared to 9.0% for E85.

The impact of this operating strategy on performance is further explained in Figure 14, which shows thermal efficiency, power, and fuel consumption as functions of CR for E85 and RG at maximum power at 1500 RPM. For E85, operating condition 1 is used for maximum power at each CR. Because of knock limitations for RG, operating condition 1 can only be used at CR=9.2, necessitating that operating condition 5 be used at CR=11.85, and that operating condition 9 be used at CR=12.87. Thermal efficiency for both fuels increases as CR increases, but the increases for E85 are much larger than for RG. The less substantial increases in efficiency for RG can be attributed to the need to switch to lower efficiency operating conditions (conditions 5 and 9) as CR increases, and having a knock-limited spark advance at these conditions. Power increases for E85 at higher CR, but decreases for RG due to the need to switch to de-rated operating conditions because of knock limitations. The result

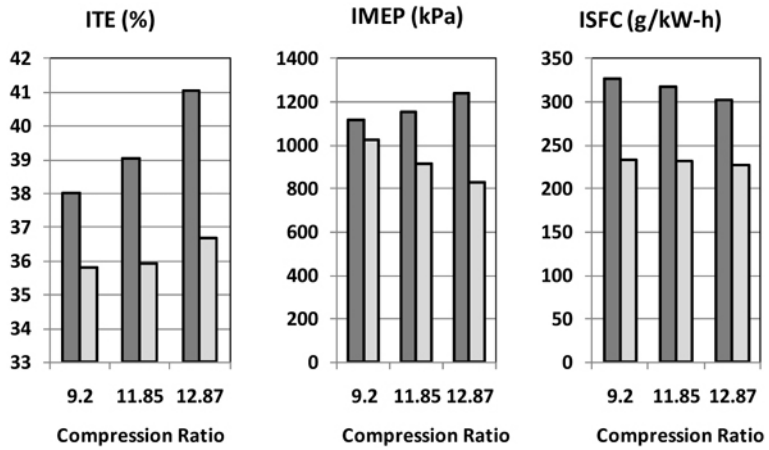

Figure 14. ITE, ISFC, and IMEP for (■) E85 and (□) RG as a function of CR at 1500 RPM and maximum power.

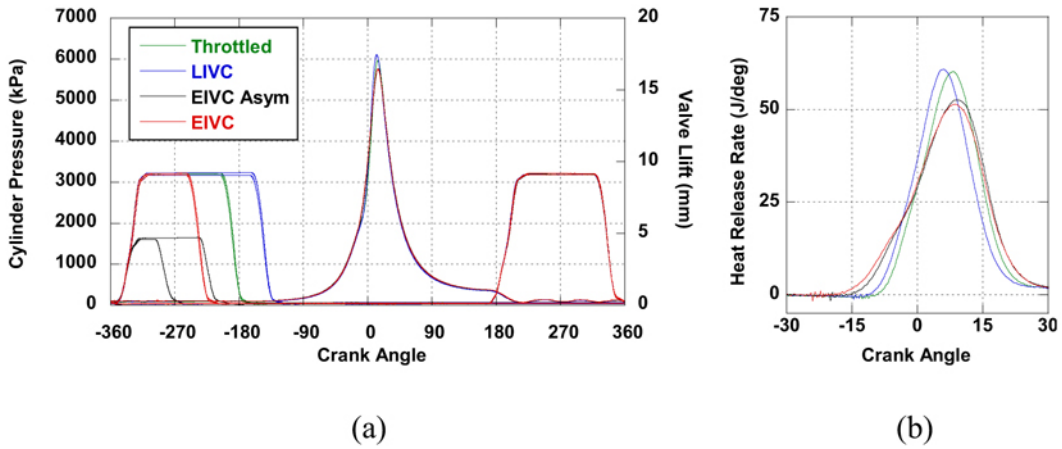

Figure 15. (a) Cylinder pressure and valve lift and (b) heat release rate for E50, CR = 11.85, for operating condition 4 (1500 rpm, 90kPa throttled), operating condition 5 (1500 rpm LIVC, 90 kPa equiv), operating condition 6 (1500 rpm EIVC, 90 kPa equiv), and operating condition 7 (1500 rpm EIVC Asym, 90 kPa equiv).

is that RG is de-rated by 8% at CR = 9.2, by 21% at CR = 11.85, and by 33% at CR = 12.87.

The third chart in Figure 14, fuel consumption as a function of CR, reveals the effect of the stated goal of this research project: the ability to reduce the fuel economy gap between E85 and conventional gasoline in an FFV. Fuel consumption decreases for both E85 and RG as CR increases, but the decrease in fuel consumption is much more significant for E85. The net result is that the fuel economy gap between E85 and RG is reduced by about twenty percent when CR is increased from 9.2 to 12.87. Thus, this operating strategy is capable of making a substantial fuel consumption improvement for E85 compared to RG at a maximum load condition.

<figure 14 here>

Combustion Analysis

The use of the LIVC and EIVC combustion strategies to control engine load have an impact on the combustion process. Figure 15 shows cylinder pressure and valve lift for E50 at CR = 11.85 and 1500 rpm for intake pressure throttled to 90 kPa (operating condition 4), and the three operating strategies using EIVC and LIVC with equivalent air flow (operating conditions 5, 6, and 7). Although each case generates an equivalent air flow, there are major variations in the valve control strategies. These differences can significantly impact combustion duration and phasing, as is shown in the heat release rate in Figure 15 (b).

<figure 15 here>

To better illustrate these operating strategies, Figure 16 shows the mass fraction burned (MFB) timing for each of the points shown in Figure 15. The point at which 50% of the

fuel is burned, or MFB 50, shows little variation with each operating strategy, which is to be expected because each strategy is operated at MBT spark timing. Table 3 can be consulted to show that the EIVC, and to a lesser extent the EIVC Asym strategies require a significantly earlier spark advance than the other strategies. The 10-90% combustion duration, or the difference between MFB 90 and MFB 10, is longest for the EIVC condition at 22 CA, followed by the EIVC Asym strategy at 20 CA, and roughly equal for the throttled and LIVC conditions at 17 CA.

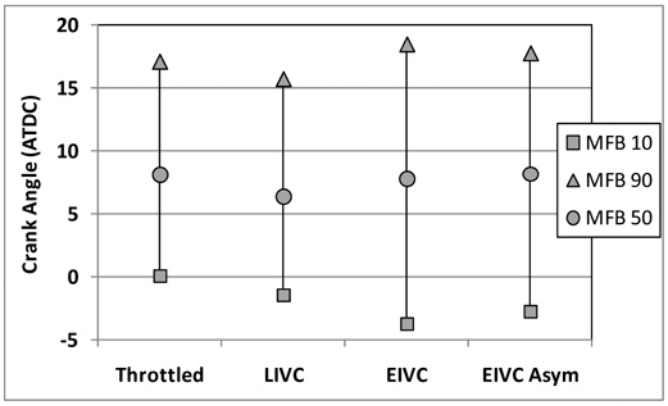

Figure 16. Combustion phasing and duration for E50 at operating conditions 4-7 (1500 rpm, 90 kPa or equiv, multiple valve operating strategies).

The reduction in combustion duration between EIVC and EIVC Asym suggests that the long combustion duration for these valve strategies is related to charge motion. We theorize that by closing the intake valves early and then drawing a vacuum on the cylinder contents before compression begins, there is a significant reduction in charge motion in the cylinder compared to the throttled or LIVC cases. Further, we conjecture that by imposing an asymmetry on the valve events with the EIVC Asym condition, we increase charge motion in the cylinder, which speeds up combustion and reduces combustion duration, as is shown in Figure 16. An earlier investigation by Cleary and Silvas [6] noted a similar trend of increased combustion duration with EIVC operation but attributed it to a lower in-cylinder temperature, which is a result of lower effective CR. However, the data from this study doesn't support that the lower temperature is the primary cause of the longer combustion duration because the LIVC condition also has a lower effective CR and is subject to a similar temperature reduction as the EIVC case, but doesn't exhibit a similar long combustion duration.

The primary impact of fuel composition on combustion phasing and duration occurs when some of the fuels have a knock-limited spark advance. Figure 17 shows combustion timing and duration for each fuel at operating condition 8 (1500 rpm, throttled 80 kPa intake) at CR = 9.2, 11.85, and 12.87. The CR = 9.2 points are the same as are shown in Figure 8. At CR = 9.2, all of the fuels behave similarly, with minimal differences in the phasing of MFB 10, 50, or 90. More of a difference is evident at CR = 11.85, where the spark advance is knock-limited for RG, HO, and E10, necessitating retarded spark and combustion phasing. The duration of the latter portion of combustion (i.e. MFB 50-90) is shortened because of a small amount of knock for these points. E50 and E85 at CR = 11.85 exhibit little difference from CR = 9.2. Finally, at 12.87, the combustion duration for E50 and E85 show little variation compared to the other CR conditions. However, the other three fuels are all knock-limited, necessitating that the spark advance be retarded, and very short MFB 50-90 duration because of a small amount of knock.

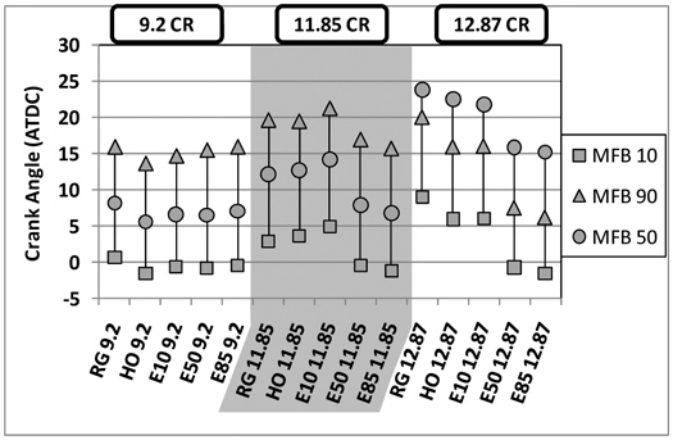

Figure 17. Combustion timing and duration for operating condition 8 (1500 rpm, throttled 80 kPa) for each fuel at CR = 9.2 and 11.85.

Thus, at a given operating condition, the primary factor affecting combustion phasing and duration is knock-limited spark advance. Increases in CR increase the likelihood of knock, but there is otherwise a minimal effect. A correlation between spark retard and efficiency has been proposed by Heywood [13], and its application here estimates a 5% penalty in output for RG when spark timing is retarded 12 degrees from MBT. Using spark retard beyond this level results in further decreases in power and increases in fuel consumption. To minimize the fuel consumption penalty, it is advantageous to lower the effective CR with either an EIVC or LIVC valvetrain strategy to maintain better combustion phasing. Peak output is also reduced using an EIVC or LIVC strategy, but the resulting fuel penalty is minimized.

DISCUSSION

The above results show that by operating with a high mechanical CR it is possible to increase engine efficiency with fuels that are not knock-limited (i.e. E85 and E50). In addition, it is possible to maintain compatibility and good efficiency with lower octane fuels that are knock-limited by

either retarded spark timing or using an EIVC or LIVC valve strategy. A retard in spark timing incurs both an efficiency and power penalty, and has a limited authority for eliminating knock at high CR. The EIVC and LIVC strategies provide a methodology that allows a larger degree of authority. There is a minimal efficiency penalty associated with these operating conditions compared to WOT conditions, and an efficiency benefit compared to an equivalent throttled operation. Another possible option to eliminate knock is exhaust gas recirculation (EGR). Similar to the EIVC and LIVC strategies, using EGR reduces the volumetric efficiency of the engine, thus the maximum power is de-rated. A comparison between EGR and the EIVC and LIVC cases is the subject of a possible future investigation.

If one considers vehicle level optimization for ethanol fuels, there are additional opportunities for higher efficiency. We have shown that E85 can deliver more power than RG at a given engine speed. One can envision a scenario where a transmission would need to downshift with RG to deliver the necessary power, but could remain in a higher gear E85. There would be, of course, an additional fuel penalty associated with the higher engine speed for RG if a transmission downshift is necessary. Another example of how E85 may provide an additional efficiency advantage is through its lower exhaust temperature. Engine calibrations use a fuel enrichment technique to lower the temperature of the exhaust at high loads in order to protect exhaust system components from thermal damage, imposing a fuel consumption penalty. Figure 18 compares the exhaust temperatures of E85 and RG at two load conditions (2500 rpm WOT and 80 kPa throttled). The exhaust temperature of RG is higher than E85 by 20-30°C at conditions where spark advance is not knock-limited. During knock-limited operation for RG, spark timing is retarded and the temperature difference with E85 increases to as much as 100°C. A higher CR reduces exhaust temperature except for cases when the spark advance is severely limited. Thus, because the exhaust temperature of E85 is significantly lower than RG, fuel enrichment to cool the temperature of the exhaust is not needed as frequently, giving E85 an additional efficiency advantage on a vehicle system level. Quantifying these effects on real-world fuel economy for E85 and gasoline under various driving cycles and transmission configurations is beyond the scope of the current study.

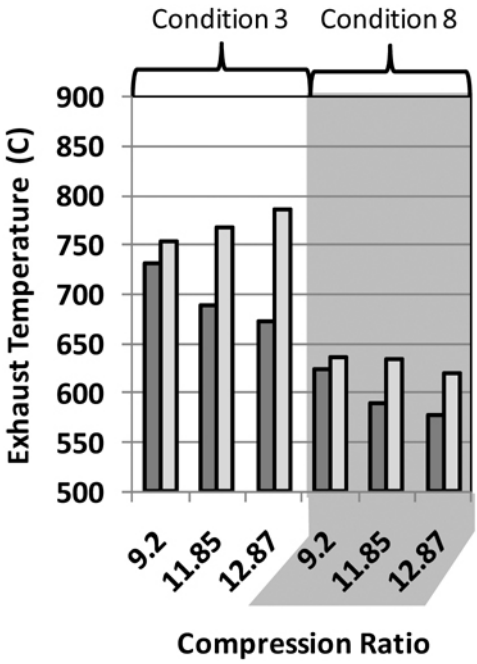

Figure 18. Exhaust temperature for (■) E85 and (□) RG as functions of compression ratio for operating condition 3 (2500 WOT) and operating condition 8 (80 kPa throttled).

As stated in the introduction, this work is part of a broader program aiming to take advantage of the unique fuel properties of ethanol. Included in the broader program is the development of a flex-fuel multi-cylinder engine with multiple cam profiles and a wide range of cam phasing authority to enable it to operate under EIVC and LIVC conditions using a cam-based valve-train. GT-power modeling software was used to simulate the engine with increased CR and is being reported separately in reference [20]. Valve-train control strategies to control effective CR and reduce throttling losses were extensively modeled to identify an approach that allowed higher CR for E85 while still maintaining flex fuel capability on regular gasoline. Based on this information, a multi-cylinder engine has been built and is undergoing test. The results of on-engine verification and optimization will be presented in a future paper.

CONCLUSIONS

A study is presented that experimentally investigates the effects of ethanol, CR, and EIVC and LIVC valve strategies at knock-prone conditions in a direct-injection engine. The major conclusions are as follows:

• Indicated thermal efficiency and IMEP both increase at higher CR, so long as the spark advance is not knock-limited. The high-ethanol content fuels (E85 and E50) are not knock-limited under any operating conditions investigated, whereas the two gasolines and the E10 become knock-limited with

increasing CR. Under knock-limited conditions, retarding spark timing incurs an IMEP penalty, which can result in a net efficiency decrease at high CR.

• At substantially similar engine conditions, thermal efficiency and engine power both increase with increasing ethanol content, even when none of the fuels are knock-limited. Contributing factors to the higher power are a charge cooling effect and a higher energy content of a stoichiometric mixture per unit mass of air, which together, account for more than 50% of the increased power. Contributing factors to the increased efficiency are explored and include a mole multiplier effect and differences in γ. The mechanisms and the relative contributions of these efficiency effects are currently being studied.

• Compatibility with knock-prone fuels can be maintained at high CR with the use of EIVC or LIVC strategies. These strategies reduce effective CR, which reduces the likelihood of knock. Compared to spark retard, this methodology provides a greater ability to maintain compatibility with knock-prone fuels at high mechanical CR configurations, and does so without a substantial efficiency penalty.

• When an EIVC or LIVC control strategy is used to prevent knock at high engine load, the engine output is substantially de-rated compared to fuels that do not exhibit knock under conventional valve timing (i.e. E85 or E50). As CR increases, knock-prone fuels become more de-rated, so much so that at CR = 12.87, the IMEP difference between E85 and RG is nearly 33%.

• The fuel consumption penalty associated with E85 can be reduced by 20% by operating at a high mechanical CR and utilizing the EIVC and LIVC control strategies to maintain compatibility with gasoline.

• Combustion duration increases with the EIVC control strategy, and is attributed to a reduction in charge motion. Asymmetric valve events can induce some additional charge motion, which decreases combustion duration. To the extent that charge motion is induced here with asymmetric valve events, combustion duration continues to be longer than the throttled and LIVC cases.

ACKNOWLEDGMENTS

This research was supported by the US Department of Energy (DOE) Office of Vehicle Technology under the fuels technologies program with a DOE management team of Kevin Stork and Dennis Smith. It is also performed under cooperative research and development agreement (CRADA) no. NFE-07-00722 between UT-Battelle, LLC and Delphi Automotive Systems LLC.

AUTHOR DISCLAIMER

REFERENCES

1. United States Energy Information Association, Official ethanol consumption statistics. URL: http://tonto.eia.doe.gov/dnav/pet/pet_pnp_oxy_dc_nus_mbbl_a.htm. Accessed on September 4, 2009.

2. One Hundred Tenth Congress of the United States of America. Energy Independence and Security Act. 2007. URL: http://frwebgate.access.gpo.gov/cgi-bin/getdoc.cgi?dbname=110_cong_bills&docid=f:h6enr.txt.pdf. Accessed on September 10, 2009.

3. ASTM D 5798-09b. "Standard Specification for Fuel Ethanol (Ed75-Ed85) for Automotive Spark-Ignition Engines." ASTM International, 2009.

4. Bechtold R., Thomas J.F., Huff S.P., Szybist J.P., Theiss T.J., West B.H., Goodman M., Timbario T.A.. Technical Issues Associated with the Use of Intermidiate Ethanol Blends (>E10) in the U.S. Legacy Fleet: Assessment of Prior Studies." Oak Ridge National Laboratory Technical Report, August 2007, ORNL/TM-2007/37. URL: https://portal.ornl.gov/sites/apps/PTS/PtsDocs/Publication%207767.pdf. Accessed on September 14, 2009.

5. Marriott, C.D, Wiles, M.A., Gwidt, J.M., Parrish. S.E., "Development of a Naturally Aspirated Spark Ignition Direct-Injection Flex-Fuel Engine," *SAE Int. J. Engines* 1(1): 267-295, 2008.

6. Cleary, D. and Silvas, G., "Unthrottled Engine Operation with Variable Intake Valve Lift, Duration, and Timing." SAE Technical Paper 2007-01-1282, 2007.

7. Mallikarjuna, J.M. and Ganesan. V., "Theoretical and Experimental Investigations of Extended Expansion Concept for SI Engines," SAE Technical Paper 2002-01-1740, 2002.

8. Smith, J.M., Van Ness H.C., Abbot M.M.. Introduction to Chemical Engineering Thermodynamics, Fifth Edition. McGraw-Hill. New York, NY. 1996. p 283.

9. Heywood, J.B. Internal Combustion Engine Fundamentals. McGraw-Hill. New York, NY. 1988. p 842-843.

10. Caton, P.A., Hamilton, L.J., and Cowart, J.S., "An Experimental and Modeling Investigation into the Comparative Knock and Performance Characteristics of E85, Gasohol [E10] and Regular Unleaded Gasoline [87 (R+M)/2]." Society of SAE Technical Paper 2007-01-0473, 2007.

11. Nakata, K., Utsumi, S., Ota, A., Kawatake, K. et al., "The Effect of Ethanol Fuel on a Spark Ignition Engine," SAE Technical Paper 2006-01-3380, 2006.

12. Stein, R.A., House, C.J., and Leone, T.G., "Optimal Use of E85 in a Turbocharged Direct Injection Engine," *SAE Int. J. Engines* 2(1):670-682, 2009.

13. Ayala, F.A., Gerty, M.D., and Heywood. J.B., "Effects of Combustion Phasing, Relative Air-fuel Ratio, Compression Ratio, and Load on SI Engine Efficiency," SAE Technical Paper 2006-01-0229, 2006.

14. Nakama, K., Kusaka, J., and Daisho. Y., "Effect of Ethanol on Knock in Spark Ignition Gasoline Engines," *SAE Int. J. Engines* 1(1):1366-1380, 2008.

15. West, B.H., López, A.J., Theiss, T.J., Graves, R.L. et al., "Fuel Economy and Emissions of the Ethanol-Optimized Saab 9-5 Biopower," SAE Technical Paper 2007-01-3994, 2007.

16. Çengel, Y.A., Boles M.A.. Thermodynamics: An Engineering Approach Fourth Edition. McGraw Hill. Boston, MA., p 864. 2002.

17. Smith, J.M., Van Ness H.C., Abbot M.M.. Introduction to Chemical Engineering Thermodynamics, Fifth Edition. McGraw-Hill. New York, NY. 1996. p 638.

18. Sezer, İ., Altin İ., Bilgin A.. "Exergetic Analysis of Using Oxygenated Fuels in Spark-Ignition (SI) Engines." Energy & Fuels, 2009, vol 23, pp 1801-1807.

19. Gallo, W.L.R. and Milanez., L.F., "Exergetic Analysis of Ethanol and Gasoline Fueled Engines," SAE Technical Paper 920809, 1992.

20. Hoyer, K., Moore, W., and Confer, K., "A Simulation Method to Guide DISI Engine Redesign for Increased Efficiency using Alcohol Fuel Blends," SAE Technical Paper 2010-01-1203, 2010.

CONTACT INFORMATION

James P. Szybist
szybistjp@ornl.gov

Wayne R. Moore
Wayne.Moore@Delphi.com

The Engineering Meetings Board has approved this paper for publication. It has successfully completed SAE's peer review process under the supervision of the session organizer. This process requires a minimum of three (3) reviews by industry experts.

ISSN 0148-7191

doi:10.4271/2010-01-0619

SAE Customer Service:
Tel: 877-606-7323 (inside USA and Canada)
Tel: 724-776-4970 (outside USA)
Fax: 724-776-0790
Email: CustomerService@sae.org
SAE Web Address: http://www.sae.org
Printed in USA